The Global Atmosphere and Ocean System, 1994, Vol. 2, pp. 121–142
Reprints available directly from the publisher
Photocopying permitted by license only

THE EFFECT OF SEA SPRAY ON SURFACE ENERGY TRANSPORTS OVER THE OCEAN

C. W. FAIRALL[1], J. D. KEPERT and G. J. HOLLAND[2]
[1] *Wave Propagation Laboratory, Boulder, Colorado, USA*; [2] *Bureau of Meteorology Research Centre, Melbourne, Australia*

(*Received November 5, 1993; in final form November 5, 1993*)

Strong winds associated with severe weather over the ocean introduce substantial amounts of spray into the lowest few meters of the atmosphere by bursting air bubbles in whitecaps and by whipping spume from the tips of waves. The presence of high concentrations of liquid water could have a substantial effect on the transfer of energy to and from the ocean surface in severe weather phenomena such as tropical cyclones. Although observational difficulties have prevented adequate direct measurements, data controlled by the former USSR oceanographic fleet over several years and occasional observations from single cyclones indicate that the lowest 100 m of the atmosphere may be cooled by over 5 K in winds above 25 m s^{-1}. A recent analytic study by Betts and Simpson also indicated that evaporation of rainfall could be the major contributor to the boundary layer thermodynamic budget.

We present an initial investigation of some of these effects for atmospheric conditions typical of those found in tropical cyclones. A parameterisation in terms of bulk meteorological quantities of the fluxes of heat and moisture to the atmosphere from the evaporation of oceanic spray droplets is developed and applied to an axisymmetric slab model of the tropical cyclone boundary layer. We show that the presence of spray has a major and realistic effect on the model solution structure and that without spray the boundary layer evolves in an unrealistic manner. The effects of rain evaporation are also considered, and are shown to be potentially of a similar magnitude to those of sea spray.

KEY WORDS: Air-sea fluxes, sea spray, tropical cyclones.

1. INTRODUCTION

The interaction between severe weather and the ocean results in several changes to both (Figure 1). Strong winds generate high seas, a layer of ocean spray, upwelling, and mixing. Rainfall may affect wave generation, and leave a long-lived lens of fresh water. These changes feed back to change the atmospheric boundary by modifying the air-sea exchange of momentum, heat and moisture. The evaporation of falling rain also moistens and cools the boundary layer.

A major source of uncertainty in the air-sea interaction in severe weather lies in determining the effect of spray, which can greatly modify the transfer of momentum, heat, and moisture, and thus the degree of development of the features illustrated in Figure 1. Water can be transferred from the ocean to the atmosphere by direct evaporation of the sea surface or, at high wind speeds, by the evaporation of sea spray. Above the droplet evaporation zone, the droplet component of the transfer takes the form of an enhanced turbulent flux of water vapor and a correspondingly reduced turbulent flux of sensible heat. Because the droplets ejected from the water are at the sea surface temperature, they also transfer sensible heat to the atmosphere in an amount directly proportional to the air-sea temperature difference.

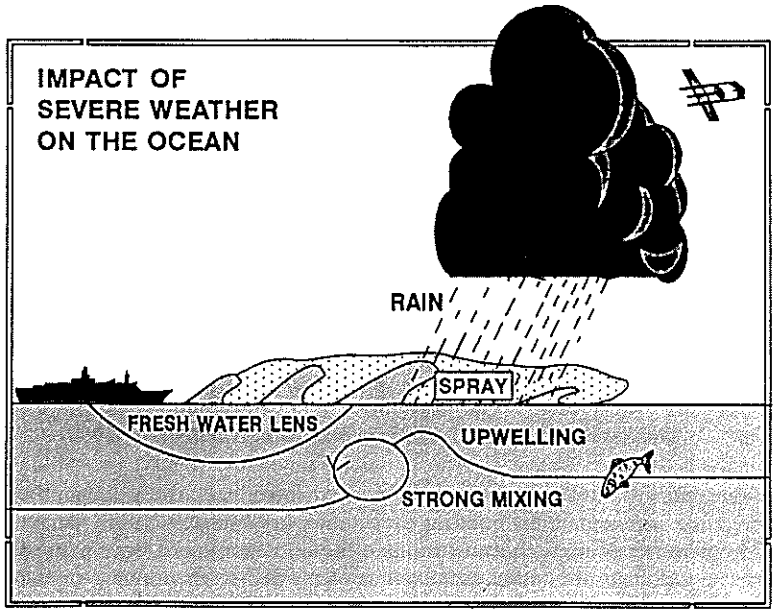

FIGURE 1 Schematic showing the major processes that modify the air-sea interaction occurring during passage of a severe weather system.

To characterise droplet mediated modification of latent and sensible heat fluxes, we must know the surface source spectrum of the sea spray, the height of the droplet evaporation zone, the vertical dispersion characteristics of the droplets, their microphysical transfers of moisture and heat to the air, and droplet interactions that modify mean temperature and moisture profiles in the evaporation zone. Furthermore, we must know how these parameters and processes change with increasing wind speed.

Present-day technology does not permit direct measurement of most of these processes over the open ocean. Measurements of the near-surface turbulent fluxes over the ocean at wind speeds in excess of $20\,m\,s^{-1}$ are quite rare, and to date only exploratory measurements of the mean fields have been attempted in the evaporation zone at sea (Ling et al., 1980; de Leeuw, 1986). Research in this area has tended to focus on laboratory simulations (wind-wave tanks) and numerical modelling (see Rouault et al., 1991 for a summary). Both Lagrangian droplet trajectory (Edson and Fairall, 1992) and one-dimensional ensemble average (Ling et al., 1980; Rouault et al., 1991) model approaches have been developed, but they have so far been applied primarily to laboratory simulations rather than realistic oceanic situations (see Rouault and Larsen, 1990, for an exception).

Tropical cyclones provide a convenient family for study of some of the bulk effects of spray. These systems are known to be markedly dependent on the exchange of energy at the ocean surface for their existence (see Frank, 1988; Holland, 1988 for a summary), and some of the most severe consequences to coastal populations arise from the high waves and strom surge that are produced. Observations indicate that substantial modifications of the boundary layer during a cyclone may be being experienced in the high wind region (Figure 2). These observations were taken by an oceanographic

research vessel of the former USSR during Typhoons "Skip" and "Tess" in November 1988. Considerable care was taken to ensure that the temperature measurements were not contaminated by wetting of the instruments. This included the use of several thermometers fitted with droplet traps. Data was discarded when differences in temperature between instruments suggested wetting and occurred. In addition, at least one instrument was equipped with a photocell to detect the entry of droplets into the thermometer enclosure. If this occurred the data was again discarded. In Figure 2, it is clear that the lowest layer of the atmosphere shows marked cooling once the winds exceed $15\,m\,s^{-1}$. One atmospheric sounding obtained at a wind speed of $18\,m\,s^{-1}$ (not shown) indicates that this cooling may extend to 100 mm height.

Although the models described above can provide detailed information on profiles of droplet concentrations, interactions and feedbacks with the mean fields, and modifications of the turbulent flux profiles within and above the evaporation zone, they are still under development and are too detailed and computationally burdensome for direct application to tropical cyclone modelling. We are undertaking a study aimed at using numerical models to investigate the broad influences that spray has on the oceanic and atmospheric boundary layer in tropical cyclones. In this paper, we report on the development of a parameterisation of the thermodynamic effects of spray and rainfall into a mesoscale model, and indicate the scale of the impact in a simple, bulk model of a tropical cyclone boundary layer. The spray parameterisation is derived in section 2. Section 3 contains details of the bulk cyclone boundary layer model and rainfall parameterisation, and the impact of spray and rainfall is discussed with a series of experiments in section 4. Our conclusions are presented in section 5.

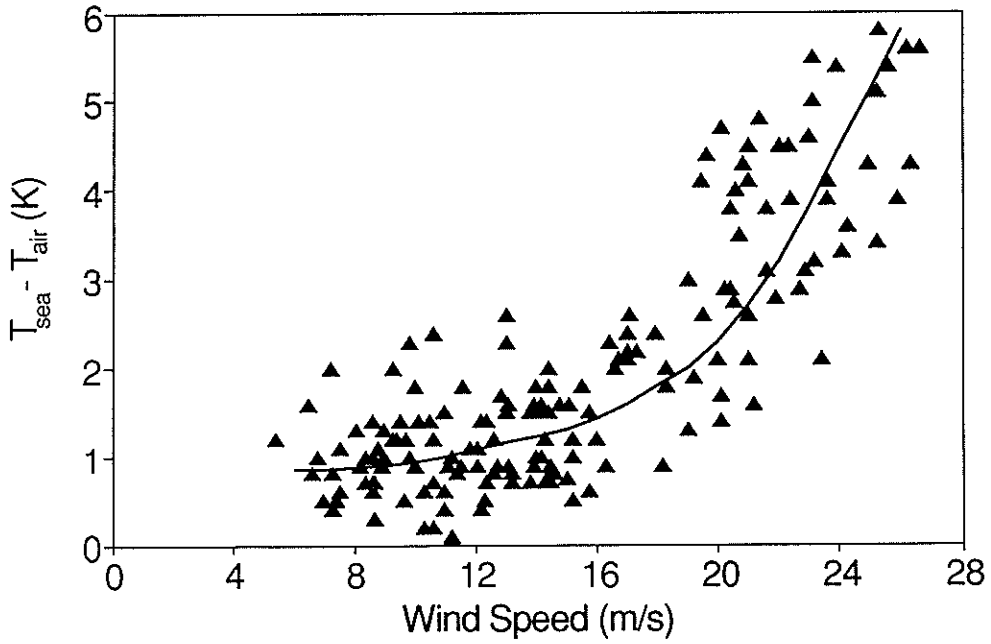

FIGURE 2 The marine boundary layer cooling associated with strong winds in two tropical cyclones, shown as a scatter diagram of observed air-sea temperature difference plotted against wind speed (Pudov, personal communication, 1991).

2. PARAMETERISATION OF SEA-SPRAY EFFECTS

In this section we develop a simple parameterisation of the sensible and latent heat fluxes provided by sea spray droplets. Our parameterisation is based on a physically-based scaling model derived from arguments about the important variables involved. Only individual scaling components, such as wind speed dependence of whitecap coverage and of the mean wave height, are derived empirically. This is a simplified and generalised derivative of an approach developed by Andreas (1992), hereafter referred to as A92, who carried out detailed computations of droplet-mediated heat fluxes for several sets of specific conditions. The parameterisation is defined only in terms of the standard bulk meteorological variables (mean wind speed, air-sea temperature difference, and relative humidity) that are available in numerical models.

2.1 Background

A92 has provided an implicit assessment of the total sensible heat transfer, Q_s, and the total latent heat transfer, Q_l, caused by the ejection and evaporation of sea spray droplets, derived from computations of the droplet temporal response times for the transfer of sensible heat, τ_s, and latent heat, τ_l. He argues that the fraction of the total potentially realisable energy transferred from a specific droplet is

$$\text{fraction} = 1 - e^{-\tau/\tau_f}$$

$$\tau_f = \frac{h}{V_f} \tag{1}$$

where τ_f is the mean droplet exposure time to the atmosphere, h is the evaporation zone scale height, and $V_f(r)$ is the gravitational fall velocity of the droplet and r is the droplet radius. The evaporation zone scale height is crudely defined as the height above the mean sea surface below which 67% of the total droplet evaporation takes place. Both measurements (de Leeuw, 1986, 1987, 1990) and modeling studies (Ling and Kao, 1976; Edson, 1990) confirm that the proper scaling height for the droplet evaporation zone is the mean wave height. For simplicity, we will take this to be the equilibrium wave height, which is a known function of wind speed. Because the energy transfer fraction is a function of radius, the total contributions to Q_s and Q_l are obtained by integrating the fraction over the droplet mass source function. For example, for a wind speed of $u = 20\,\text{m s}^{-1}$, a water temperature of $T_s = 302\,\text{K}$, an air temperature of $T_a = 300\,\text{K}$, and a relative humidity of $RH = 0.80$, A92 found a droplet mediated latent heat flux of $170\,\text{W m}^{-2}$ versus a direct latent heat flux of $380\,\text{W m}^{-2}$, using the droplet size distribution given by his Figure 3.

2.2 Scaling Model Simplifications

Rather than perform the detailed time-scale calculations and integrals over the droplet spectrum, as per A92, for each time step and grid point in our hurricane model, we wish to simplify the computations of Q_s and Q_l to a single parameterisation in bulk variables. It is not that we consider the A92 computations impractically time consuming, but

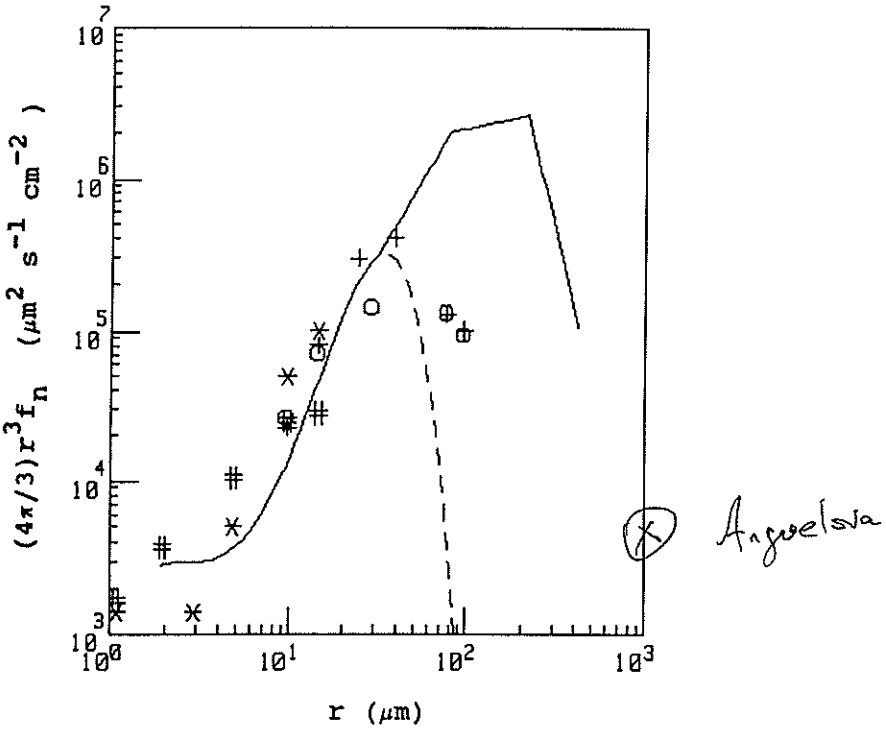

FIGURE 3 Whitecap normalized droplet surface source function in volume flux format versus droplet radius. The symbols represent the following data sources: o and +, Edson (1989); *, Miller and Fairall (1988); and #, Woolf et al. (1988). The dashed line represents the bubble component parameterisation and the solid line represents the combined bubble and spume component parameterisations.

rather that the final influences of the droplets are still too uncertain to justify this complexity at this stage of our investigation. We note the spume droplet portion of the flux spectrum is still speculative and that when the droplet mediated fluxes become comparable to the direct fluxes, there will certainly be modifications of the mean fields and the turbulent fluxes in and above the evaporation zone. A simple parameterisation will also make it clear how the droplet mediated fluxes scale with wind speed and air-sea bulk differences.

To begin, we define the droplet source number density spectrum, $s_n(r)$, as the number of droplets of radius, r, ejected into the atmosphere each second per unit area of sea surface per radius increment. The subscript n indicates that s represents the number of droplets whereas subscripts A or V used later indicate droplet area or volume. Also, we use lower-case s to indicate the droplet spectrum whereas upper-case S represents a property that is an integral over radius. The combined effect of the size-spectrum of droplets is obtained by adding up the individual effect of each size droplet, taking into account the relative numbers of each size—in other words, integrating over the entire spectrum.

The source spectrum depends on wind speed. Because heat and moisture require different integral properties, the simplest parameterisation requires that we separate the meteorological conditions from the integral over the source-size spectrum. With this simplification, the radius integral need be evaluated only once and the meteoro-

logical variability is carried explicitly by the remainder of the scaling expressions. We make two simplifications that allow us to do this.

First, we assume that the source function, $s_n(r)$, is similar at all wind speeds and is proportional to the whitecap areal fraction, $W(u)$. The validity of this approximation is discussed by Fairall (1990) and is supported by the source functions given in A92. We express the source spectrum as

$$s_n(r) = W(u) f_n(r) \tag{2}$$

where $f_n(r)$ is the source spectrum per unit area of whitecap. The function used is an average of $s_n(r)/W(u)$ obtained from the combined bubble droplet source function of Miller (1988) and the spume droplet function of Wu et al. (1984), as described by A92. The form of $f_n(r)$ is shown if Figure 3. We use

$$W(u) = 3.8 \times 10^{-6} u^{3.4} \tag{3}$$

from Monahan and O'Muircheartaigh (1980). This has a stronger wind speed dependence than some more recent evaluations (O'Muircheartaigh and Monahan, 1986; Spillane et al., 1986) and may overestimate the droplet effects when extrapolated beyond $20\,\mathrm{m\,s^{-1}}$. However, Spillane et al. (1986) suggest a form almost the same as Equation 3 for warm water, which we deem appropriate for our purposes.

The second simplification is based on the observation that mass flux (as depicted in Figure 3) is dominated by droplets with radii in the range of 20 to 400 μm. An examination of A92's computations of the three time scales of these droplets shows that for this droplet size range

$$\frac{\tau_s}{\tau_f} \ll 1 \tag{4a}$$

$$\frac{\tau_l}{\tau_f} \gg 1 \tag{4b}$$

Equation 4a implies that all relevant droplets will be able to transfer their excess sensible heat to the atmosphere before falling back into the water. Thus, the droplet mediated sensible heat flux contribution is proportional to the mass flux, F_m, and the air-sea temperature difference, $T_s - T_a$,

$$Q_s = c_{pw} F_m (T_s - T_a), \quad F_m = \rho_w W(u) S_v, \quad S_v = \int_0^\infty \frac{4\pi}{3} r^3 f_n(r)\, dr. \tag{5}$$

Here ρ_w and c_{pw} are the density and specific heat of liquid water. Note that A92 uses the wet bulb temperature, T_w, rather than T_a in his definition of Q_s. We prefer to allocate to the latent heat the additional heat flux associated with the droplet cooling from T_a to T_w. Evaluation of S_v from Figure 3 is straightforward and yields $S_v = 5.0 \times 10^{-6}\,\mathrm{m\,s^{-1}}$, which is independent of meteorological conditions.

2.3 Droplet Evaporation

Using the above approach, we can express the *potential* evaporation flux, E_p, for the droplets as

$$E_p = L_e F_m \tag{6}$$

where L_e is the latent heat of vaporisation of water. E_p is the latent heat flux that would result if all spray droplets evaporated before impacting the ocean and would be the correct flux if $\tau_l \ll \tau_f$. Because equation 4 applies, we must take a different approach. We begin by considering the rate of loss of mass by evaporation, e, by a single droplet of radius r (Pruppacher and Klett, 1978, equations 13.6 and 13.50),

$$e = -4\pi F_p D_v \rho_a r(q_p - q) \tag{7}$$

where D_v is the diffusivity of water vapor, ρ_a the density of air, q the ambient specific humidity, and q_p the saturation specific humidity at the droplet temperature. As the mass flux is dominated by droplets with $r > 10\,\mu$m, we take D_v to be constant and neglect non-continuum ("slip") effects (Pruppacher and Klett, pp. 322–323). F_p is the droplet ventilation factor,

$$F_p = 1 + 0.25\left(\frac{2V_f r}{v}\right)^{0.5} \tag{8}$$

where v is the kinematic viscosity of air.

Note that equation 4a implies that the droplet is at the wet bulb temperature for most of its exposure to the atmosphere but equation 4b implies that e and r are essentially constant. We take V_f to vary linearly with radius,

$$V_f = 8000\,r = ar \tag{9}$$

which is in close agreement with the formula in Pruppacher and Klett (1978, pp. 323–324 and Figure 10–20) for the droplet size range of interest here.

The total loss rate of liquid water by evaporation at some point within the evaporation zone is obtained by integrating equation 7 over the number concentration of the droplets, $n(r)$,

$$-\frac{dq_l}{dt} = \int e\,n(r)dr = \rho_a(q_p - q)S'_a \tag{10}$$

where

$$S'_a = 4\pi D_v \int F_p r n(r)dr \tag{11}$$

To evaluate equation 11, we need to specify $n(r)$ within the evaporation zone. We assume that the droplet concentration is uniform with height below h (Edson, 1990) and negligible above. In practise there are droplets above h, but the evaporation from these should be compensated by reduced evaporation in the high humidity region near the surface. Therefore, the vertical flux of droplets is simply $n(r)\,V_f$, which must be in balance with the surface production flux (Fairall et al., 1983).

$$n(r)\,V_f = W(u)f_n(r). \tag{12}$$

Again, we can separate the meteorological variables from the integral over the droplets

$$-\frac{dq_l}{dt} = \rho_a W(u)S_a(q_p - q) \tag{13}$$

with S_a given by

$$S_a = \frac{S'_a}{W(u)} = 4\pi D_v \int \frac{F_p(r) r f_n(r)}{V_f(r)} dr. \tag{14}$$

Of the droplet size range we are considering, the smaller droplets go closest to violating equation 4b; that is, they go closest to achieving moisture equilibrium before they fall back into the sea. A92 showed that the contribution of these droplets to the overall water vapor flux is minor, but we run the risk here of overestimating their effect. This is illustrated by the fact that the value of the integral in equation 14 is somewhat sensitive to the choice of lower bound. We choose a lower bound of 23 μm for the integral, giving $S_a = 0.125\,\mathrm{s}^{-1}$, so that equation 13 agrees with the exact calculations of A92.

It is interesting to note that the integrand in equation 14 decreases with increasing r, so that S_a depends more upon the source function for droplets with $r < 100\,\mu$m than on larger ones. We will eventually see that the droplet-mediated moisture flux is proportional to S_a, and it is encouraging that the most uncertain part of our source function does not contribute as strongly to S_a as the better known parts.

Equation 13 defines the rate of evaporation of the droplets (in $\mathrm{kg\,m^{-3}\,s^{-1}}$) at some location above the sea surface. The apparent turbulent water-vapor flux at some height above the evaporation zone, F_q, is the integral of equation 13 from the surface to the top of the evaporation zone. Although we have claimed that the droplet concentration is roughly constant in the evaporation zone, $q_p - q$ approaches 0 at the surface. We assume that the integral of $q_p - q$ can be approximated as $h[q_p(h) - q(h)]$, where h is the mean wave height. Thus, the loss of evaporation below the mean wave height is assumed to be compensated by increased evaporation for droplets carried higher by waves larger than h and by turbulent diffusion. The flux of water vapor above the evaporation zone resulting from the evaporation of droplets is

$$F_q = h\rho_a W(u) S_a (q_p - q). \tag{15}$$

This result implies that the droplet contribution to the moisture flux is proportional to the total surface area of sea spray droplets per unit area of sea surface.

Finally, we must account for the fact that the droplets are maintained at the wet bulb temperature rather than the air temperature. We use the droplet thermal exchange equation from Pruppacher and Klett (1978, equation 13.61) to express the wet bulb depression:

$$T_w = T_a - \frac{L_e D_v}{c_{pa} D_T}[q_s(T_w) - q] \tag{16}$$

where c_{pa} is the specific heat of air, D_T is the heat diffusivity, and q_s denotes the saturation specific humidity. Using the Clausius-Clapeyron relation, we expand the saturation specific humidity, subtracting q from both sides, to get

$$q_s(T_w) - q = q_s(T_a) - q + \frac{\varepsilon L_e}{RT^2}(T_w - T_a)\, q_s(T_a) \tag{17}$$

where $\varepsilon = 0.622$ and R is the gas constant for dry air. Combining equations 16 and 17 yields

$$q_s(T_w) - q = \beta[q_s(T_a) - q] \tag{18}$$

where, assuming $D_v/D_t = 1$, β is given by

$$\beta = \left[1 + \frac{\varepsilon L_e^2}{R c_{pa} T^2} q_s(T_a)\right]^{-1} \tag{19}$$

Values for β range from 0.59 at 273 K to 0.21 at 303 K.

The final expression for the droplet mediated flux is

$$Q_l = S_a W(u) h(u) \beta(T_a) \rho_a L_e [q_s(T_a) - q] \tag{20}$$

We specify the mean wave height by (Kinsman, 1965, p. 391; Wilson, 1965; Earle, 1979)

$$h(u) = 0.015 u^2. \tag{21}$$

Both the $W(u)$ and $h(u)$ parameterisations used here are based on u defined as the mean wind speed at a height of 10 m.

2.4 *Profile Adjustments*

Two additional factors must be considered to obtain our final expressions for the droplet mediated fluxes. In equations 5 and 20, our parameterisations for $h(u)$ and $W(u)$ use coefficients appropriate for the wind speed at 10 m, which is consistent with standard bulk conventions. However, the values for T_a and q are defined at height h and so we need to determine a correction factor such that we can use the 10 m values. The high wind conditions would normally allow us to assume logarithmic profiles for the specific humidity and replace $q(h)$ with $q(10)$, except that the presence of evaporating droplets voids the necessary assumption of constant flux. However, Rouault and Larsen (1990) and Rouault et al. (1991) suggest the departure is sufficiently small that we may write

$$q_s(T_s) - q(h) \approx [q_s(T_s) - q(10)]\left(1 - \frac{C_e^{0.5}}{k} \ln \frac{10}{h}\right) \tag{22}$$

where $k = 0.4$ is the von Karman constant. We assume that this correction also applies approximately to $q_s(T_a)$ and obtain

$$q_s(T_a(h)) - q(h) = \gamma(u)\,[q_s(T_a(10)) - q(10)], \quad \gamma(u) = 1 - 0.087 \ln \frac{10}{h} \tag{23}$$

We also apply this factor to the air-sea temperature difference in the Q_s expression of equation 5, and will henceforth use T_a and q at the standard reference height.

The second profile issue concerns the ultimate fate of the moisture and heat liberated from the droplets. We cannot assume that all of Q_s and Q_l appear at the top of the evaporation zone. Smith (1990) indicated that the droplet evaporation will perturb the normal log profiles of mean q and T in the evaporation zone, leading to a reduction in latent heat flux and an increase in sensible heat flux below h, but vice versa above h. This

new equilibrium structure of both the mean and turbulent flux profiles has been verified by numerical simulations (Rouault and Larsen, 1990; Rouault et al. 1991). We illustrate this structure in Figure 4.

We anticipate that only a fraction, α, of Q_l will be realised above the droplet zone. Assuming a reference height well above the evaporation zone, H_l computed by standard methods is then a poor representation of the true latent heat flux, which should be $H_l + \alpha Q_l$. Note that the actual evaporative cooling of the ocean is $H_l - (1-\alpha)Q_l$ because of increased moisture near the sea surface. However, this lost cooling is compensated by the increased sensible heat $H_s + (1-\alpha)Q_l$ being removed from the ocean to evaporate the droplets. The numerical simulations (Roualt and Larsen 1990 and Rouault et al., 1991) show that $\alpha \approx 0.5$, even for massive droplet fluxes as high as $E_p = 12{,}500\ \mathrm{W\,m^{-2}}$. Incorporating this factor, the final expressions for the droplet mediated fluxes are then

$$Q_s = 0.5 S_v W(u)\gamma(u)\rho_w c_{pw}(T_s - T_a)$$
$$Q_l = 0.5 S_a h(u) W(u)\gamma(u)\beta(T_a)\rho_a L_e[q_s(T_a) - q] \tag{24}$$

2.5 *Comparison to Standard Bulk Transfer Processes*

Putting in the various constants and writing equation 24 in terms of atmospheric density and heat capacity yields

$$Q_s = 3.2 \times 10^{-8} u^{3.4}\gamma(u)\rho_a c_{pa}(T_s - T_a) \tag{25a}$$
$$Q_l = 3.6 \times 10^{-9} u^{5.4}\gamma(u)\beta(T_a)\rho_a L_e[q_s(T_a) - q] \tag{25b}$$

with u in $\mathrm{m\,s^{-1}}$.

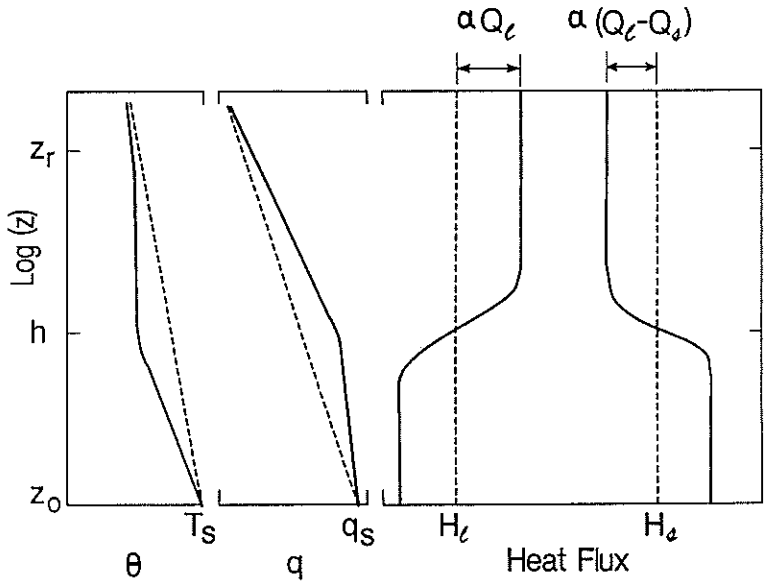

FIGURE 4 Near-surface structure of q, θ, and the heat fluxes. The dashed lines represent the undisturbed structure in the absence of droplets, the solid lines represent the equilibrium structure after modification by evaporating droplets. The factor α characterises the fraction of total droplet contribution actually realised above the evaporation zone after profile modification.

To set this in context, let us first state the standard bulk expressions for the direct, turbulent fluxes

$$H_s = \rho_a c_{pa} C_h u (T_s - \theta_r)$$
$$H_l = \rho_a L_e C_e u [q_s(T_s) - q(z_r)] \tag{26}$$

where C_h and C_e are the bulk transfer coefficients for sensible and latent heat and θ_r is the potential temperature at the reference height, relative to the surface pressure, computed from T_a. Note that

$$\theta_r \approx T_a(z_r) + 0.0098 z_r$$
$$q(z_r) = RH(z_r)\, q_s(T_a(z_r)) \tag{27}$$

where z_r is the reference height for the specification of the wind speed, air temperature, and relative humidity. For a reference height of 10 m, C_e and C_h are approximately 1.2×10^{-3} and have little wind speed dependence (Liu et al., 1979; Smith, 1988). We can now compute the ratios of droplet mediated and bulk fluxes, $f_s = Q_s/H_s$ and $f_l = Q_l/H_l$

$$f_s = 2.7 \times 10^{-5} u^{2.4}$$
$$f_l = 3.0 \times 10^{-6} u^{4.4} \beta(T_a) \frac{q_s(T_a) - q}{q_s(T_s) - q}. \tag{28}$$

We have ignored the distinction between the air-sea difference of temperature and potential temperature and have for the moment dropped the $\gamma(u)$ factor, which varies only between 0.90 and 1.08 for u between 15 and 40 $\mathrm{m\,s^{-1}}$.

Figure 5 shows a comparison of equation 28 at various wind speeds with the calculations taken from Figure 9 of A92. We have divided A92's values by two because he did not consider the evaporation layer profile adjustment process. Note that Q_l becomes significant compared to H_l (20%) at a wind speed of about 15 $\mathrm{m\,s^{-1}}$; Q_s becomes significant compared to H_s at a wind speed of about 40 $\mathrm{m\,s^{-1}}$. Furthermore, an examination of A92's Table 3, which contains computations of fluxes for $u = 20\,\mathrm{m\,s^{-1}}$, shows that

$$Q_l[q_s(T_a) - q]/\beta(T_a) \simeq \text{constant} \tag{29}$$

for water temperatures ranging from 273 to 302 K and air temperatures ranging from 263 to 300 K.

2.6 *Range of Applicability*

For application in numerical models, the normal bulk heat fluxes are computed from the lowest atmospheric level in the conventional manner. The droplet mediated fluxes are computed using equations 24 or 25a, b. The lower flux boundary conditions for the atmosphere are then given by

$$\text{Sensible Heat: } H_s + Q_s - Q_l$$
$$\text{Latent Heat: } H_l + Q_l \tag{30}$$

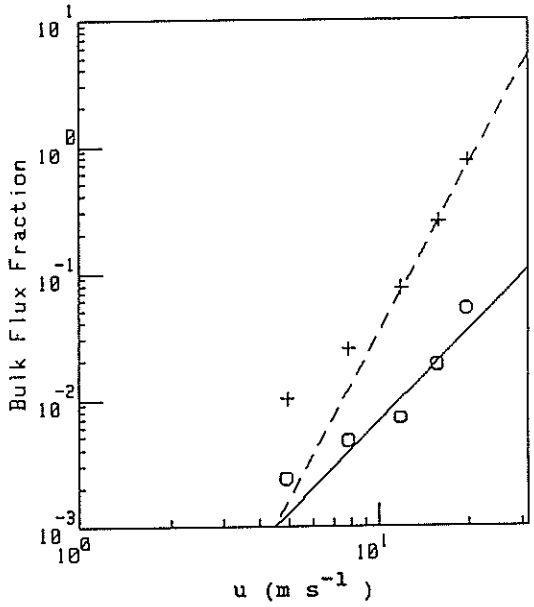

FIGURE 5 The ratio of droplet mediated to bulk fluxes as a function of wind speed: equation 25 compared with the computations from A92. For latent heat flux, f_l, ($T_a = 273.06$ K, $T_s = 273.16$ K, and $RH = 0.80$) the plus symbols are from A92 and the dashed line is from equation 25. For sensible heat flux, f_s ($T_a = 263.16$, $T_s = 273.16$, and $RH = 0.80$) the circles are from A92 and the solid line is from equation 25.

Noting that $Q_s \ll Q_l$, the total oceanic surface energy boundary condition is not changed. Equation 30 thus also implies that the flux of moist static energy (or equivalent potential temperature) is not changed by droplet evaporation but the surface balance is modified toward a cooler, moister boundary layer.

The whitecap fraction and droplet flux spectrum parameterisations are based on measurements taken at wind speeds up to about 25 m s^{-1}, so this must be considered the strict limit of applicability of the final parameterisation. At the upper end of the strict limit of applicability, droplet evaporation is about 20% of direct bulk evaporation (depending on conditions) but the cooling effects of the droplet evaporation will be much larger than the droplet mediated sensible heat flux. Because we have taken a physical approach to the parameterisation, we expect to be able to extrapolate to higher wind speeds (albeit with decreasing confidence). At about 28 m s^{-1}, the droplet contribution is comparable to the direct turbulent flux. Therefore, it is of interest to ponder the logical limits to this extrapolation.

At a wind speed of 40 m s^{-1}, equation 3 yields a whitecap fractional area of 1.0. We do not expect the whitecap fraction to exceed 1.0, but we do expect the droplet production to continue to increase with wind speed in an unknown manner. Two other parameterisation assumptions also begin to break down near 40 m s^{-1}. Our assumption that r and e are constant is equivalent to assuming that $Q_l/E_p \ll 1$. At 40 m s^{-1}, Q_l/E_p is approximately 0.33 at an RH of 0.80. Obviously E_p is a strict upper limit on Q_l [which can be violated by equation 25b]. Finally, our assumption that the mean wave height represents an upper limit on the vertical distribution of the droplets breaks down when the turbulence is sufficiently intense to transport droplets well above the

production region. Toba (1965) has shown this limit is reached when $u > V_f/(k\,C_u^{0.5})$, where C_u is the velocity drag coefficient. Thus, for u greater than about 50 m s^{-1} sea-spray droplets will be vertically transported well into the boundary layer and truly staggering boundary-layer export processes will be required to prevent rapid saturation.

In conclusion, we suggest that equation 30 can be used with wind speeds up to about 30 m s^{-1} (whitecap fraction of about 0.5). Using it for winds above 40 m s^{-1} is likely to be fraught with peril.

Incidently, we can also conclude that the droplets make an insignificant contribution to the surface stress in this wind speed range. Assuming that the droplets are ejected with negligible horizontal velocity but acquire the mean wind speed, u, before reimpacting the sea surface, they will increase the momentum transfer. We can compute the ratio of the droplet contribution to the standard bulk stress as

$$f_t = F_m \frac{u}{\rho_a C_u u^2} = 8 \times 10^{-6} u^{2.4} \tag{31}$$

which is about 0.1 at $u = 50$ m s^{-1}. This is at variance with the results of Pielke and Lee (1990), who show a significant impact on the surface wind profile due to spray droplet mass loading. We believe the discrepancy is due to the high values of water mass loading they use, ranging from 0.032 kg m^{-3} to 0.32 kg m^{-3}, when averaged over the lowest 10 m. Our parameterisation gives a mass loading of

$$\int \frac{4}{3}\pi r^3 \rho_w n(r) dr = \frac{4}{3}\pi \rho_w W(u) \int \frac{r^3 f_n(r)}{V_f(r)} dr$$

which is 0.0029 kg m^{-3} at 30 m s^{-1}, increasing to 0.0077 kg m^{-3} at 40 m s^{-1}. Thus even the least of their water loadings due to spray is an order of magnitude too large. Although the droplet source function is not well known, A92 rejects a source function which produces many more spume droplets than ours on the grounds that it leads to unrealistically high values of spray sensible and latent heat fluxes.

3 APPLICATION TO TROPICAL CYCLONES

3.1 Model Formulation

As a test of the parameterisation in section 2, and to provide a preliminary estimate of the relative importance of droplet and conventional fluxes in an important real-world situation, a simple model of the tropical cyclone boundary layer was developed. This model is axisymmetric and assumes the hurricane boundary layer to be well mixed. It is formulated with potential temperature θ and specific humidity q as prognostic variables, and integrated until a steady state is reached. The boundary layer depth z_i, is defined as the cloud base height and velocity components u and v are prescribed and fixed.

The budget equations are

$$\frac{\partial \theta}{\partial t} = -u\frac{\partial \theta}{\partial r} + \frac{\overline{w'\theta'}_0 - \overline{w'\theta'}_{z_i}}{z_i} - \frac{L_e E}{\rho c_p z_i} \tag{33}$$

and

$$\frac{\partial q}{\partial t} = -u\frac{\partial q}{\partial r} + \frac{\overline{w'q'}_0 - \overline{w'q'}_{z_i}}{z_i} + \frac{E}{\rho z_i} \tag{34}$$

where the terms containing E define the effects of rainfall evaporation and are described more fully in the next section.

The direct surface fluxes are calculated by a modified Liu-Katsaros-Businger (1979, henceforth LKB) algorithm. Three modifications are made:

(i) Combining the formulae of LKB and Charnock (1955) for the roughness length to obtain $z_0 = 0.011u_*^2/g + 0.11\nu/u_*$, where ν is the kinematic viscosity, as suggested by Smith (1988).

(ii) Altering the dependence on stability of the profiles of temperature, moisture and momentum in highly unstable conditions $z_r/L < -5$ (where z_r is the boundary layer reference height and L is the Monin-Obukhov length) to

$$\psi_T = \frac{3.22}{2.57}\left(1.5\ln\frac{y^2+y+1}{3} - \sqrt{3}\tan^{-1}\frac{2y+1}{\sqrt{3}} + \frac{\pi}{\sqrt{3}}\right) \tag{35}$$

and

$$\psi_U = \frac{2.05}{2.57}\left(1.5\ln\frac{y^2+y+1}{3} - \sqrt{3}\tan^{-1}\frac{2y+1}{\sqrt{3}} + \frac{\pi}{\sqrt{3}}\right) \tag{36}$$

where

$$y = \sqrt[3]{1 - 12.87 z_r/L} \tag{37}$$

This is readily derived by integrating the 1/3 power law expression $\phi_T = \phi_U = (1-\gamma z/L)^{-1/3}$ for the dimensionless gradients, which has the proper free convection form (Panofsky and Dutton; 1984, pp. 133–144) and is thus more appropriate for such highly unstable conditions than the Businger-Dyer formulae used by LKB.

(iii) Modifying equation 2b of LKB to

$$\frac{(T - T_s)}{T_*} = \frac{\left(\ln\frac{z_r}{z_T} - \alpha_H\psi_T\right)}{\alpha_H k} \tag{38}$$

with a similar change to equation 2b of LKB. The value $\alpha_H = \alpha_Q = 1.18$ is used to be consistent with the von Karman constant of 0.4 we are using here.

Equation 25 is used for the droplet mediated fluxes. To prevent the latent heat flux exceeding the total mass of droplets available for evaporation, it is modified to $1/(1/Q_l + 1/E_p)$.

The top fluxes are given by

$$\overline{w'\theta'}_{zi} = -(\Theta - \theta)w_e \tag{39}$$

and

$$\overline{w'q'}_{zi} = -(Q - q)w_e \tag{40}$$

where the equation for the entrainment velocity

$$w_e = \max\left(0.2\frac{\overline{w'\theta_0'}}{\Theta_v - \theta_v}\left(1 + 3.2\left(\frac{-L}{z_i}\right)\right), 0\right) \tag{41}$$

incorporates the suggestion of Fairall (1984) to account for the effects of shear generated turbulence along with those of the surface buoyancy flux, but does not include the effects of cloud downdrafts. Here, upper-case variables Θ and Q denote free atmosphere values immediately above the boundary layer. The model formulation is summarized in Figure 6.

Space derivatives are calculated by a centred finite difference scheme, and the time step is implicit, giving essentially the Crank-Nicholson algorithm. A 1-2-1 filter is applied every ten time steps to prevent the growth of $2\Delta r$ wavelength noise. The inner boundary condition of $u = 0$ at $r = 0$ means the field at the centre point is affected only by the local fluxes. At the outer edge of the domain (1,000 km in the following examples), either θ and q are held fixed at their initial value, or the space derivative is set to zero. This choice does not affect the model solution inside 500 km.

The sea surface temperature, free atmosphere temperature and moisture, boundary layer depth, and outer boundary θ and q (where appropriate) are prescribed.

3.2 Parameterisation of Rainfall Effects

The rainfall rate R, in a steady-state cyclone, is assumed to be equal to the local water vapor flux out of the top of the boundary layer. That is,

$$R = \rho_w(\overline{w'q'}_{z_i} + \bar{w}q) \tag{42}$$

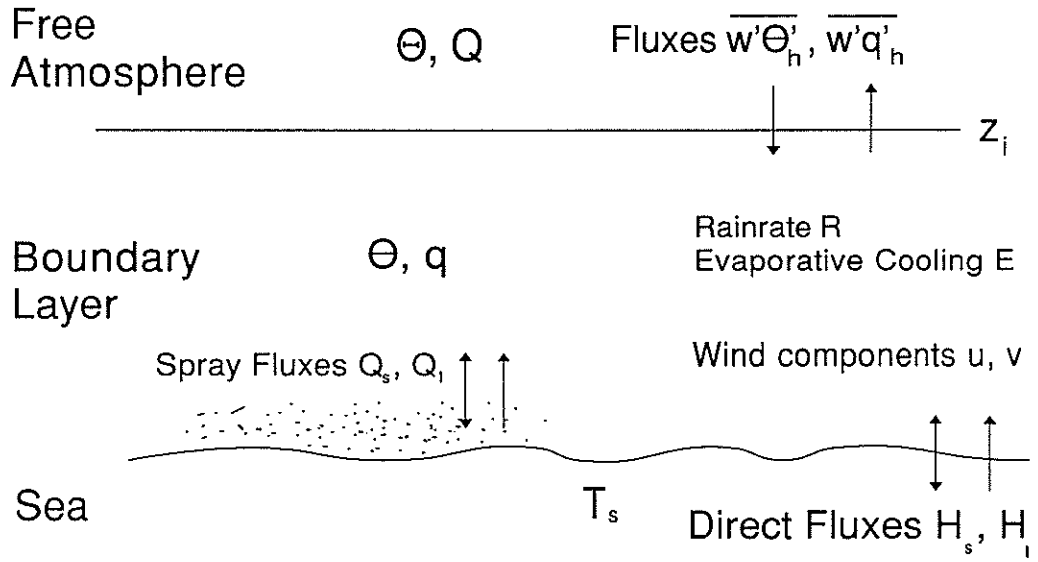

FIGURE 6 Schematic of the bulk tropical cyclone boundary layer model.

and is also by definition the vertical liquid water mass flux,

$$R = \frac{4\pi}{3}\rho_w \int_0^\infty V_f(r) n(r) r^3 dr \tag{43}$$

where $V_f(r)$ is the fall velocity of a droplet of radius r, $n(r)$ is the rain droplet size spectrum, and ρ_w is the density of liquid water.

The evaporation rate $\partial m/\partial t$ of a single rain droplet is given by equation 7. Here we approximate $F_p \simeq 0.25(2V_f r/v)^{1/2}$ as $r > 50\,\mu$m for typical raindrops, and assume the droplet temperature to be the wet bulb temperature. The total flux due to evaporation through the depth of the boundary layer is then

$$\begin{aligned} E &= z_i \int_0^\infty \frac{\partial m}{\partial t}(r)\, n(r)\, dr \\ &= 4\pi z_i D_v \rho_a \beta [q_{\text{sat}}(T) - q] \int_0^\infty F_p(r) n(r) dr \end{aligned} \tag{44}$$

where equations 18 and 19 have been used to simplify $q_{\text{sat}}(T_p) - q = \beta(q_{\text{sat}}(T) - q)$ and we have neglected the change in size of the droplets as they fall.

The ratio of evaporation rate to rainfall rate then becomes

$$\frac{E}{R} = \frac{3}{4}\left(\frac{2}{v}\right)^{1/2} z_i D_v \left(\frac{\rho_a}{\rho_w}\right) \beta [q_{\text{sat}}(T) - q] \frac{\int_0^\infty V_f(r)^{1/2} r^{3/2} n(r)\, dr}{\int_0^\infty V_f(r) r^3 n(r)\, dr} \tag{45}$$

For tropical raindrops, $r \sim 1$ mm and so we take $V_f = 10\,\text{m s}^{-1}$, and use the Marshall-Palmer raindrop size distribution $n(r) = 8 \times 10^3 \exp(-r/r_0)$ where $r_0 = 0.13 R^{0.21}$ and R is in millimeters per hour. Thus

$$\begin{aligned} \frac{E}{R} &= \frac{3}{32}\sqrt{\frac{\pi}{5v}}\, z_i D_v \frac{\rho_a}{\rho_w} \beta [q_{\text{sat}}(T) - q] r_0^{-3/2} \\ &= (1.213 \times 10^{-5}\,\text{mm}^{3/2} g^{-1} m^2) z_i \rho_a \beta [q_{\text{sat}}(T) - q] r_0^{-3/2} \end{aligned} \tag{46}$$

and this in combination with equation 42 gives E.

Probably the largest uncertainty in the parameterisation comes from the specification of the rainfall rate distribution through equation 42, which is sensitive to the assumed vertical velocity w. There is a lack of good data on cloud base vertical velocity in tropical cyclones, so here we have calculated it from the assumed radial velocity profile via the continuity equation.

4. DISCUSSION

To investigate the potential effects of spray and rainfall on the tropical cyclone boundary layer, the model was integrated to equilibrium and various combinations of

the physical processes were activated. In each case, the tangential wind profile used was the tropical cyclone bogus of Holland (1980) adjusted for a cyclone with maximum gradient level wind of $30\,m\,s^{-1}$ at a radius of 50 km and central pressure of 970 hPa. The gradient wind is adjusted to a 10 m wind for the flux calculations by multiplying by 0.8, as suggested by Powell (1980). The radial wind was prescribed as an inflow of 20° at radii greater than 100 km, going smoothly to 0 at the centre, and the boundary layer depth held fixed at 500 m. This lead to a maximum rainfall-rate of around $7\,cm\,day^{-1}$, in reasonable agreement with Frank's (1977) composite. The free atmosphere has a temperature of 303 K and a specific humidity of $16\,g\,kg^{-1}$, whilst the sea surface temperature is 301 K. Other reasonable choices of these parameters do not cause major changes to the results below. The inner 25 km of the radial profiles are not shown because the model was not designed to represent the conditions within the eye.

The first experiment contained none of the droplet processes (sea spray and rain evaporation). Because there is an inversion at the top of the boundary layer, the heat flux here is directed downward. With the comparatively weak radial flow in tropical cyclones limiting advective changes, an equilibrium is possible only if the surface heat flux is also downward; that is, if the boundary layer is warmer than the sea surface. This is, of course, contrary to the usually observed situation for tropical cyclones. To get the model to reach an equilibrium in this case, it was necessary to prescribe a free atmosphere potential temperature of 304 K, 3 K warmer than the sea surface. Further evidence of the implausibility of this configuration of the model is given in Figure 7, which shows temperature increasing markedly toward the radius of maximum wind (RMW), again in contradiction of observations.

Including the spray parameterisation produced a much more physically reasonable temperature profile (Figure 8). Note particularly the significant cooling near the RMW

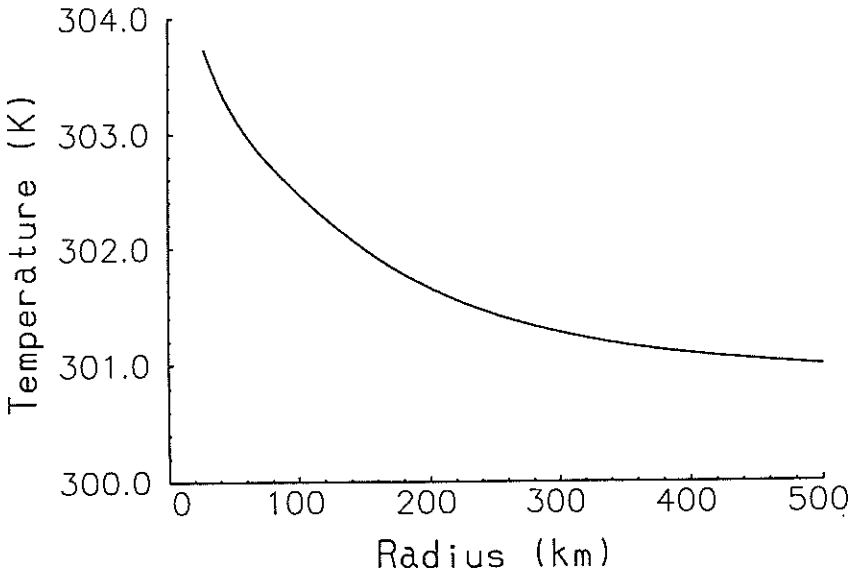

FIGURE 7 Radial profile of temperature in the model tropical cyclone boundary layer with no droplet evaporation processes. The sea surface temperature is 301 K and the free atmosphere temperature is 305 K.

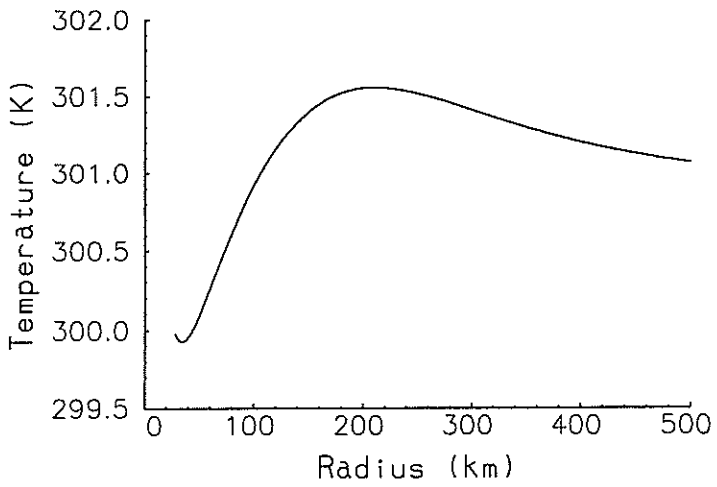

FIGURE 8 Radial profile of temperature in the model tropical cyclone boundary layer with droplet evaporation processes included. The sea surface temperature is 301 K and the free atmosphere temperature is 303 K.

due to spray droplet evaporation. Here, the downward surface sensible heat flux needed to balance the downward flux at the boundary layer top is provided by the spray, the Q_l term in equation 30 acts as a significant heat sink. This is shown clearly in Figure 9, which gives the breakdown of surface sensible and latent heat fluxes into their droplet mediated and direct components. It is seen that Q_l is about one-half H_l at the peak, but is more concentrated near the stronger winds. H_s is an order of magnitude smaller, whereas Q_s is negligible at these relatively modest wind speeds.

Another process that could produce the boundary layer cooling needed to balance the warming by downward sensible heat flux at the boundary layer top is evaporation of rain. Including the rain parameterisation produced a slightly cooler boundary layer (Figure 10) than that produced by ocean spray (Figure 8). Increased cooling resulted from inclusion of both sea spray and rain (Figure 10), giving a somewhat cooler boundary layer than spray alone. The air-sea temperature difference thus produced is at the low end of the range suggested by the observations in Figure 2.

Given the lack of good experimental data on the spray source function and hence Q_l, it is appropriate briefly to consider the sensitivity of the model to varying the magnitude of Q_l. Accordingly, the above "spray only" and "rain and spray" experiments were repeated with Q_l being halved and doubled. In the "spray only" case, doubling Q_l produced an additional 0.5 K of cooling at the RMW, whilst halving it all but eliminated the air-sea temperature difference. This latter case was, however, still some 3 K cooler than the "no rain or spray" case. The impact on the "rain and spray" case was less, amounting to about 0.1 K in either direction. This was due to the moister boundary layer in this case reducing the potential for further evaporative cooling.

These results suggest that sea spray droplet evaporation may be important in the maintenance of the cyclone boundary layer. They are, however, preliminary in that several important effects are at present omitted from the model, and they should therefore be treated with due caution. The model is being extended to include

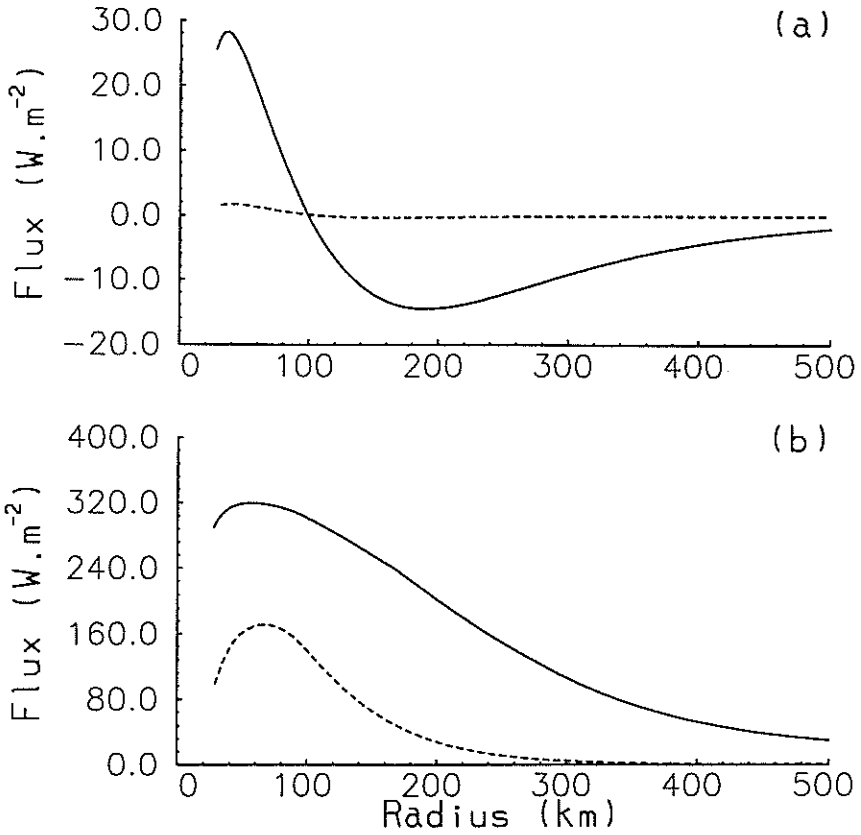

FIGURE 9 Relative contributions of direct (solid lines) and sea spray (dotted lines) evaporation processes to the surface sensible (upper panel) and latent heat (lower panel) fluxes, for the experiment in Figure 8.

a calculated boundary layer depth and the effect of cloud base fluxes of heat and moisture, as well as the momentum budget, and this work will be the subject of a forthcoming paper (Kepert, 1993). The cloud base fluxes, in particular, are expected to play an important role. Further work is also needed to clear up the relative importance of sea spray and rain evaporation. This distinction contains important implications for the overall dynamics of the boundary layer, since the vertical distribution of cooling, and hence the static stability, will be very different in the two cases. For example, if the cooling is dominated by spray and therefore confined to the lowest 100 m or so of the boundary layer, the resulting increase in stability would be expected to reduce significantly the surface momentum transfer. This would affect storm surge forecasts, and could also allow inertial oscillations to develop with the concomitant formation of a low level jet above the cooled layer.

The results were compared with the boundary layer budget of Betts and Simpson (1986). In our notation, the surface flux figures averaged over the annulus from radius 30 km to 90 km from their Table 3a are $H_s = 228\ \mathrm{W\,m^{-2}}$, $Q_s = 110\ \mathrm{W\,m^{-2}}$, $H_l = 1578\ \mathrm{W\,m^{-2}}$ and $Q_l = 1788\ \mathrm{W\,m^{-2}}$. The relative magnitudes of the various terms are broadly similar. Closer agreement would not be expected as their cyclone is significantly stronger than the one here, and this model does not as yet include the important cloud base processes present in their calculations.

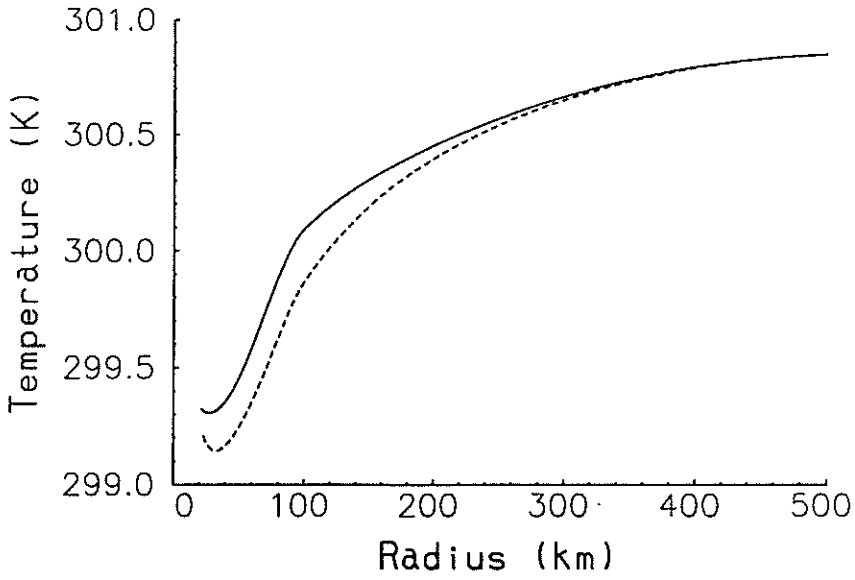

FIGURE 10 Radial profile of temperature in the model tropical cyclone boundary layer with rain drop evaporation only (solid line) and sea spray and rain evaporation (dashed line). The sea surface temperature is 301 K and the free atmosphere temperature is 303 K.

5. CONCLUSIONS

The contribution of ocean spray and rainfall to the thermal structure of a tropical cyclone boundary layer has been investigated. First we developed parameterisations of the effects of spray and rainfall in terms of bulk meteorological parameters. The spray parameterisation draws on recent work by de Leeuw (1986, 1987, 1989), Ling and Kao (1976), and Edson (1990) in assuming that spray droplets are injected at the wave height, and of Andreas (1992) in assuming that the droplets adjust rapidly to the wet bulb temperature, but fall back into the ocean before they have lost a large proportion of their mass. In this parameterisation, the contributions of oceanic spray to air-sea fluxes become comparable to direct fluxes at wind speeds above about $20\,m\,s^{-1}$ for moisture, and above about $35\,m\,s^{-1}$ for sensible heat. We are confident in the physics of the parameterisation up to $30\,m\,s^{-1}$, and believe it to be reasonable up to $40\,m\,s^{-1}$. It is, however, dependent on the droplet source function used and should be modified as more data becomes available on this. Beyond that, other processes will become important as droplets are turbulently transported through the full depth of the boundary layer.

These parameterisations were incorporated into a simple axisymmetric slab model of the tropical cyclone boundary layer, and the sensitivity of the model to sea spray and raindrop evaporation was examined. We found that a highly unrealistic structure developed without the inclusion of droplet processes. Including either or both of sea-spray or rain parameterisation led to a more realistic hurricane surface temperature profile, albeit with detail differences between the different calculations. We reiterate our earlier cautions about the simplicity of the present model.

The study indicates that the effect of spray and rainfall on the boundary layer structure under high wind conditions may be large and cannot be ignored. The analytic

results agree with the findings of Betts and Simpson (1987) that evaporation has a major impact on the hurricane boundary layer. Our results are also supported by observations from two typhoons collected by the former USSR oceanographic fleet (Pudov, personal communication, 1991).

These findings indicate that care needs to be taken with use of simple boundary layer models and concepts in developing theories of tropical cyclone development and maximum intensity. Further analytic work is planned, first with a more sophisticated slab boundary layer model, then with a full primitive equations model with resolved boundary layer. A major limitation, however, will be the lack of direct observations.

Acknowledgments

Many thanks to Mike Manton and Jim Edson for helpful discussions on this topic. The data in Figure 2 was kindly provided by Vladimir Pudov. Partial support for this research has been provided by the US Office of Naval Research through grant N-0014-89-J1737 and the US National Oceanic and Atmospheric Administration Climate and Global Change Program.

References

Andreas, E.L. (1992) Sea spray and the turbulent air-sea heat fluxes. *J. Geophys. Res.*, **97C**, 11429–11441.

Betts, A.K. and Simpson, J. (1987) Thermodynamic budget diagrams for the hurricane subcloud layer. *J. Atmos. Sci.*, **44**, 842–849.

Charnock, H. (1955) Wind stress on a water surface. *Q. J. R. Meteorol. Soc.*, **84**, 443–447.

de Leeuw, G. (1986) Vertical profiles of giant particles close above the sea surface. *Tellus*, **38B**, 51–61.

de Leeuw, G. (1987) Near-surface particle size distribution profiles over the North Sea. *J. Geophys. Res.*, **92**, 14631–14635.

de Leeuw, G. (1990) Profiling of aerosol concentrations, particle size distributions, and relative humidity in the atmospheric surface layer over the North Sea. *Tellus*, **42B**, 342–354.

Earle, M.D. (1979) Practical determinations of design wave conditions. In *Ocean Wave Climate* (Eds. M.D. Earle and A. Malahoff). Plenum: New York. pp. 39–60

Edson, J.B. (1989) Ph.D. Thesis, The Pennsylvania State University.

Edson, J.B. (1990) Simulating droplet motion above a moving surface. In *Modelling the Fate and Influence of Marine Spray* (Eds. P. Mestayer, E.C. Monahan, and P.A. Beetham). Whitecap Rep. 7, University of Connecticut, Marine Sciences Institute, Groton, pp. 84–94.

Edson, J.B. and Fairall, (1992) Lagrangian model simulations of the turbulent transport of evaporating spray droplets. *J. Geophys. Res.*, (submitted).

Fairall, C.W. (1984) Wind shear enhancement of entrainment and refractive index structure parameter at the top of a turbulent mixed layer. *J. Atmos. Sci.*, **41**, 3472–3484.

Fairall, C.W. (1990) Modelling the fate and influence of marine spray. In *Modelling the Fate and Influence of Marine Spray*, (Eds. P. Mestayer, E.C. Monahan, and P.A. Beetham). Whitecap Rep. 7, University of Connecticut, Marine Sciences Institute, Groton, pp. 1–5.

Fairall, C.W. Davidson, K.L. and Schacher, G.E. (1983) An analysis of the surface production of sea-salt aerosols. *Tellus*, **35B**, 31–39.

Frank, W.M. (1977) The structure and energetics of tropical cyclones I. Storm structure. *Mon. Wea. Rev.*, **105**, 1119–1135.

Frank, W.M. (1988) Tropical cylone formation. In: *A Global View of Tropical Cyclones* (Eds. R.L. Elsberry). Office of Naval Research, Marine Meteorology Program, Arlington, VA, pp. 53–90.

Holland, G.J. (1980) An analytic model of the wind and pressure profiles in hurricanes. *Mon. Wea. Rev.*, **108**, 1212–1218.

Holland, G.J. (1988) Mature structure and structure change. *A Global View of Tropical Cyclones* (Ed. R.L. Elsberry). Office of Naval Research, Marine Meteorology Program, Arlington, VA, pp. 13–52.

Kepert, J.D. (1993) The impact of sea spray on atmospheric boundary layer structure and dynamics under tropical cyclone conditions. *J. Atmos. Sci.* (submitted).

Kinsman, B. (1965) *Wind Waves*, Prentice-Hall, Englewood Cliffs, N.J.
Ling, S.C. and Kao, T.W. (1976) Parameterization of the moisture and heat transfer process over the ocean under whitecap sea states. *J. Phys. Oceanogr.*, **11**, 324–336.
Ling, S.C., Kao, T.W. and Saad, A.I. (1980) Microdroplets and transport of moisture from the ocean. *Proc. ASCE, J. Eng. Mech. Div.*, **106**, 1327–1339.
Liu, W.T., Katsaros, K.B. and Businger, J.A. (1979) Bulk parameterization of the air-sea exchanges of heat and water vapour including the molecular constraints at the interface. *J. Atmos. Sci.*, **36**, 1722–1735.
Miller, M.A. (1988) *An investigation of aerosol generation in the marine planetary boundary layer.* MS Thesis, Department of Meteorology, Pennsylvania State University, University Park, PA.
Miller, M.A. and Fairall, C.W. (1988) A new parameterisation of aerosol generation in the marine planetary boundary layer. Paper presented at *Seventh conference on ocean-atmosphere interaction*, American Meteorological Society, Anaheim, California, Jan. 31 to Feb. 5, 1988.
Monahan, E.C. and O'Muircheartaigh, I. (1980) Optimal power-law description of oceanic whitecap coverage dependence on wind speed. *J. Phys. Oceanogr.*, **10**, 2094–2099.
O'Muircheartaigh, I. and Monahan, E.C. (1986) Statistical aspects of the relationship between oceanic whitecap coverage, wind speed, and other environmental factors. In *Oceanic Whitecaps* (Eds. E.C. Monahan, G. Mac Niocaill, and D. Reidel). pp. 125–128.
Panofsky, H.A. and Dutton, J.A. (1984) *Atmospheric Turbulence: Models and Methods for Engineering Applications*, John Wiley and Sons.
Pielke, R.A. and Lee T.J. (1991) Influence of sea spray and rainfall on the surface wind profile during conditions of strong winds. *Boundary-Layer Meteorology*, **55**, 305–308.
Powell, M.D. (1980) Evaluations of diagnostic marine boundary-layer models applied to hurricanes. *Mon. Wea. Rev.*, **108**, 757–765.
Pruppacher, H.R. and Klett, J.D. (1978) *Microphysics of Clouds and Precipitation*, (Ed. D. Reidel).
Rouault, M.P. and Larsen, S.E. (1990) *Spray droplets under turbulent conditions.* RISO-M-2845, Dep. of Meteorol. and Wind Energy, RISO National Laboratory, Denmark.
Rouault, M.P., Mestayer, P.G. and Schiestel, R. (1991) A model of evaporating spray droplet dispersion. *J. Geophys. Res.*, **96**, 7181–7200.
Smith, S.D. (1988) Coefficients for sea surface wind stress, heat flux, and wind profiles as a function of wind speed and temperature. *J. Geophys. Res.*, **93**, 15467–15472.
Smith, S.D. (1990) Influence of droplet evaporation on HEXOS humidity and temperature profiles. In *Modelling the Fate and Influence of Marine Spray* (Eds. P. Mestayer, E.C. Monahan, and P.A. Beetham). Whitecap Rep. 7, University of Connecticut, Marine Sciences Institute, Groton, pp. 171–174.
Spillane, M.C. Monahan, E.C., Bowyer, P.A., Doyle, D.M. and Stabeno, P.J. (1986) Whitecaps and global fluxes. In *Oceanic Whitecaps* (Eds. E.C. Monahan, G. Mac Niocaill and D. Reidel). pp. 209–218.
Toba, Y. (1965) On the giant sea-salt particles in the atmosphere, II. Theory of the vertical distribution in the 10 m layer over the ocean. *Tellus*, **17**, 365–382.
Wilson, B.W. (1965) Numerical prediction of ocean waves in the North Atlantic for December, 1959. *Dtsch. Hydrogr. Z.*, **18**, 114–130.
Woolf, D.K., Bowyer P.A. and Monahan E.C. (1987) Discriminating between the film drops and jet drops produced by a simulated whitecap. *J. Geophys. Res.*, **92**, 5142–5150.
Wu, J., Murray, J.J. and Lai, R.J. (1984) Production and distributions of sea spray. *J. Geophys. Res.*, **89**, 8163–8169.